Experimental study of the dc conductivity mechanisms in amorphous Si_xSn_{1-x} alloys

N. Maloufi, A. Audouard, M. Piecuch, M. Vergnat, G. Marchal, and M. Gerl
Laboratoire de Physique du Solide, Université de Nancy I, Boite Postale No. 239 54506 Vandoeuvre-les-Nancy Cedex, France
(Received 20 July 1987)

Amorphous alloys of composition Si_xSn_{1-x} with $x=0.47-1$ were prepared by coevaporation and condensation of the constituents on substrates held at 77 K, in a vacuum better than 10^{-8} Torr. Accurate measurements of the dc conductivity were made between the lowest temperature allowed by the technique used, i.e., 6 K for $x=0.47$ and about 50 K for $x=1$, and room temperature, in annealed samples. The small-polaron model, in its high-temperature version, is shown to correctly represent the data for $T>30$ K. Variable-range hopping models, with a density of states changing exponentially with energy in the vicinity of the Fermi level, agree with experiment in the whole range of temperature and concentration. Physical quantities such as $N(E_F)$ and the shape of the $N(E)$ curve are estimated as a function of x, and their evolution with annealing treatment is studied.

I. INTRODUCTION

Considerable interest has recently been raised by the electrical transport properties of amorphous semiconductors (*a*-Si, *a*-Ge, *a*-Si:H, etc.) prepared by different methods.[1-4] In particular the nature of charge carriers and the conductivity mechanisms involved have been studied in some detail as a function of temperature. It has been shown that the conductivity is generally thermally activated at elevated temperatures and that it loses its Arrhenius behavior at low temperatures, the differential activation energy coming down with lowering temperature.[5] Numerous models have been suggested to account for this nonactivated behavior of the dc conductivity, which can be classified in two broad categories.

(i) As the density of localized states at the Fermi level in amorphous (nonhydrogenated) semiconductors is generally large, the conductivity can be attributed to electron hopping between localized states. The individual jump frequency ω between two sites separated by the distance R has been evaluated by Miller and Abrahams[6,7] in a one-phonon model and using the deformation potential approximation to describe electron-phonon interactions:

$$\omega = u \exp\left[-\frac{\Delta}{k_B T}\right] \exp\left[-\frac{2R}{a}\right] . \tag{1}$$

In this expression, Δ is the energy difference of the two sites and the last factor arises from the transfer integral between the wave functions, of extension a, centered on the two sites, and u is a frequency factor.

At intermediate temperatures, the thermal energy is large enough for the electrons to jump towards nearest-neighbor sites, even though their energy difference Δ may possibly be large. As the temperature is lowered, the factor $\exp(-\Delta/k_B T)$ decreases and it can be advantageous for an electron to jump towards sites of low Δ, but situated at large distance. The optimization of this process leads to the well-known Mott formula[1]

$$\sigma = \sigma_0 \exp[-(T_0/T)^{1/4}] . \tag{2}$$

The expressions of the parameters σ_0 and T_0 involve $N(E_F)$, the density of states at the Fermi level but, in the initial form of Mott's formula, the values of $N(E_F)$ deduced, respectively, from the slope and intercept of the trace of $\ln\sigma$ versus $T^{-1/4}$ differ by many orders of magnitude. Percolation theory has been used to obtain a more detailed picture of the electronic transport process.[7] The system was described by an array of impedances Z_{ij} connecting the localized centers:

$$Z_{ij} = Z_{ij}^0 \exp\xi_{ij} , \tag{3}$$

where

$$\xi_{ij} = \frac{2R_{ij}}{a} + \frac{\Delta_{ij}}{k_B T} .$$

At each temperature a critical impedance $Z_c(T) = Z_0 \exp\xi_c$ is determined. Z_c is the smallest impedance for which a continuous path can be traced between the ends of the sample. The resistance of the whole system is thus determined by Z_c. This theory again leads to the $T^{-1/4}$ law [Eq. (2)] for the conductivity, and the consistency between σ_0 and T_0 is usually improved.[3,7] This is because there are dead ends in the percolation network, whereas, in Mott's theory, a carrier can always escape from a given site.

In order to improve the agreement of the theory with experiment, and in particular to explain deviations from the $T^{-1/4}$ law at low temperature the effect of a density of states that changes with energy in the vicinity of the Fermi level has been considered.[8] Finally at very low temperatures, Coulomb correlations open a gap in the density of states,[3] but the temperature below which this gap could be detected by electron transport measurements is usually much too low in amorphous semiconductors to allow experimental detection.

(ii) It has also been suggested that the nonactivated behavior of the conductivity of amorphous semiconductors at low temperature can be attributed to small polaron motion.[9-11] Even though small polarons have not been observed in crystalline silicon, it is possible that, in a

disordered system, an electron in a localized state could polarize the lattice enough to collapse into a polaronic state. The mobility of small polarons is thermally activated above the Debye temperature Θ_D.[5] At lower temperatures ($T \lesssim \Theta_D/3$) the curvature in the Arrhenius plot is attributed to the thermal variation of the individual jump frequency itself, and not to variable-range hopping. It is also possible that the distribution in energy of polaronic sites, in a disordered system, leads to variable-range hopping of the polarons.[5,12]

Most of the experimental work devoted to the mechanisms of dc conductivity in amorphous semiconductors has been made in elemental systems (*a*-Si, *a*-Ge, etc.).[13,14] As the ability of a system to form polarons depends on its electronic and elastic properties, it is interesting to investigate amorphous alloys, because their electronic parameters (optical band gap, density of localized states, etc.) can be changed with composition, annealing temperature, etc. In particular, we have shown in our laboratory[15–18] that it is possible to incorporate up to 50% of tin in silicon to form a homogeneous amorphous phase. The optical gap decreases from 1.46 to 0.50 eV when the tin concentration increases from zero to 0.50.[19] Another advantage of using Si-Sn alloys is that the conductivity increases with tin content so that the lowest temperature for which the conductivity can be experimentally measured falls down from 50 K for pure *a*-Si to about 6 K for $Si_{0.47}Sn_{0.53}$. This allows us to check the competing theories in a larger temperature and composition range than in previous studies.

The aim of the present work is to investigate the possible conduction mechanisms in amorphous Si_xSn_{1-x} alloys at low and intermediate temperature, to elucidate which mechanism is predominant and whether there is a crossover as temperature and composition are changed. This paper is organized as follows. Section II is devoted to the experimental method used for preparing amorphous Si-Sn alloys and for measuring the resistivity at low temperature, after various annealing treatments. The experimental data are given in Sec. III and analyzed in the framework of variable-range hopping (VRH) and small-polaron theories. Finally, in the discussion of Sec. IV we come to the conclusion that the VRH theory (with a variable density of states) allows us to account for the experimental data at all temperatures and concentrations investigated, whereas the polaron model fails to correctly represent the data at low temperature.

II. EXPERIMENT

Amorphous samples of the alloy Si_xSn_{1-x} with composition ranging from $x=0.47$ to $x=1.0$ were prepared by co-evaporation of silicon from an electron gun and of tin from a thermal crucible, in a vacuum better than 5.10^{-8} Torr. The rate of evaporation of each element was controlled by independent piezoelectric quartz balances. The condensation of the elements was carried out on glass substrates held at liquid-nitrogen temperature. Prior to the alloy preparation, chromium electric contacts, 500 Å thick, were deposited on the substrates. The distance between electrodes was about 10 mm. Simultaneously with the preparation of resistivity samples, some alloys were prepared on amorphous carbon films deposited on electron microscopy grids. Systematic observations were made to check that the films obtained remained amorphous when heated up to room temperature.

After preparation, the resistivity samples were heated up to 300 K at the rate 2 K min^{-1} in the preparation chamber. This treatment was made to obtain samples in a standard structural state and to avoid subsequent structural relaxation.

The resistivity measurements were carried out in a helium convection cryostat using the guard-low technique, with a HP 4140 B ammeter. This technique allowed us to measure dc currents as low as 5.10^{-13} A, which corresponds to a lowest conductivity of $\sigma \simeq 10^{-10}$ $\Omega^{-1}cm^{-1}$. More experimental details referring to this technique can be found in Ref. 20.

The influence of annealing above room temperature was also studied on samples with $x=1.0$, 0.9, and 0.75, whose crystallization temperature is much higher than 300 K.[19] The samples were annealed by heating up to the annealing temperature T_a at the rate of 2 K min^{-1}, and cooled down to room temperature. The thermal variation of their conductivity below T_a was then determined, showing the effect of structural relaxation.

III. RESULTS AND INTERPRETATION

The experimental data obtained for $x=0.47$, 0.62, 0.77, 0.90, and 1.0 are shown in Fig. 1. As discussed in the introduction, the range of temperatures for which conductivity measurements are feasible increases considerably when the tin content increases. For pure amorphous silicon it is difficult to measure σ below 50 K, whereas for $x=0.47$ it is possible to lower the temperature down to 6 K. This circumstance allowed us to check our data against different theories within a broad field of temperature and composition. In the present section we compare our data with the predictions of VRH and percolation models and with the result of the small-polaron theory.

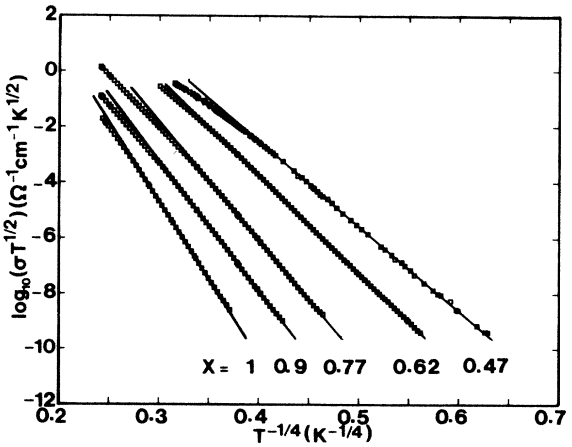

FIG. 1. Variation of $\log_{10}(\sigma T^{1/2})$ with $T^{-1/4}$ in amorphous Si_xSn_{1-x} alloys with $x=0.47$, 0.62, 0.77, 0.90, and 1. The straight lines are best fits to Mott's formula.

A. Variable-range hopping models

1. VRH theory: constant density of states

In the framework of the initial VRH model,[1] the conductivity of a disordered system can be written

$$\sigma=\sigma_0\exp[-C_3(T_0/T)^{1/4}] \quad (4)$$

with

$$k_BT_0=[a^3N(E_F)]^{-1},$$

$$\sigma_0\sim 0.1e^2(\nu/a)[a^3N(E_F)]^{1/2}(k_BT)^{-1/2},$$

where a is the localization length of the one-electron wave function in localized states, $N(E_F)$ is the density of states at the Fermi level, ν is an average phonon frequency, and C_3 is a constant close to 2. According to Eq. (4), the variation of $\log_{10}(\sigma T^{1/2})$ as a function of $T^{-1/4}$ is shown in Fig. 1.

The straight lines which correspond to linear portions of the experimental curves correctly represent the data at intermediate temperatures, but deviations are observed at high and low temperatures. High-temperature deviations can be attributed to the fact that activated processes are operating, or, in the framework of the VRH theory to the decrease of $N(E)$, with respect to $N(E_F)$, for $E\gg E_F$. The slope of the linear traces allows one to determine the product $a^3N(E_F)$ as a function of alloy composition. Figure 2 shows that this product decreases from about 8×10^{-3} eV^{-1} for $x=0.47$ to about 7.5×10^{-4} eV^{-1} in pure silicon. In order to obtain values for $N(E_F)$, the localization length a must be estimated. Measurements of $2d$-conductivity in amorphous silicon[8,13] provided values of a between 3 and 6 Å, whereas from ac conductivity data,[21] values for a between 13 and 17 Å have been obtained. In what follows the average value $a=10$ Å has been chosen and kept independent of the alloy concentration. Thus $N(E_F)$ is found to increase from 7.5×10^{17} eV^{-1}cm^{-3} for pure amorphous silicon to 8×10^{18} eV^{-1}cm^{-3} for $x=0.47$.

Using again the formula (4) with the values obtained for $a^3N(E_F)$, it is possible to obtain an estimation of the parameter ν/a, as shown by the curve labeled 1 in Fig. 3. With the choice $a=10$ Å made previously, this would lead to very large values for ν (2×10^{23} s^{-1} for pure a-Si and 4×10^{21} s^{-1} for $x=0.47$). This inconsistency with phonon frequencies is the manifestation of the well-known incompatibility of the values of $N(E_F)$ deduced from the slope and intercept in the initial expression of Mott's formula.

2. Percolation theory: variable density of states

A more detailed picture of the conductivity process is given by percolation theory. In particular Pollak *et al.*[7,8] determined the temperature dependence of the conductivity using a percolation calculation where the spatial positions and the energies of localized states are random independent variables. In Ref. 8 they consider the effect of a concave density of states of the form

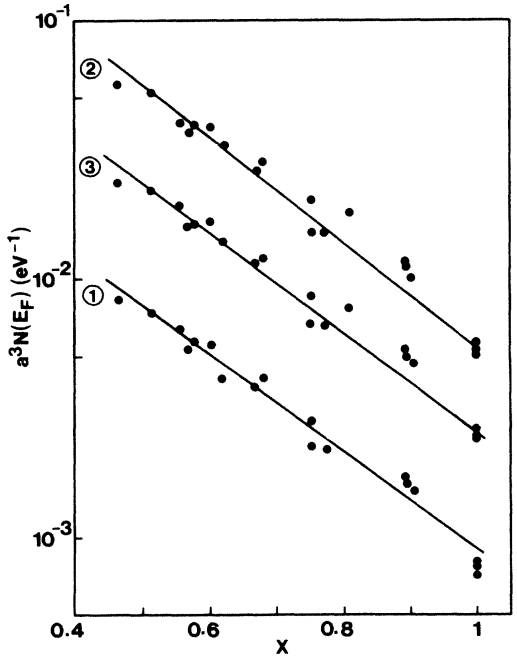

FIG. 2. Variation with x of the product $a^3N(E_F)$ in a-Si_xSn_{1-x} alloys; a is the range of localized wave functions. 1, Mott's model with a constant density of states; 2, Ortuno and Pollak's model; 3, Mott's model with an exponential density of states.

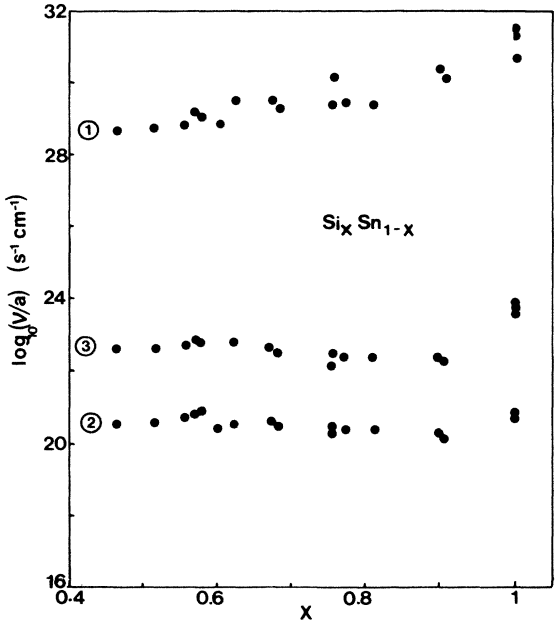

FIG. 3. Variation with x of $\log_{10}(\nu/a)$, considered as a parameter: 1, Mott's model with a constant density of states; 2, Ortuno and Pollak's model; 3, Mott's model with an exponential density of states.

$$N(E)=N(E_F)\exp(E/E_0)\ , \tag{5}$$

where E_0 is an energy parameter. At the percolation threshold the equation

$$f(y)=(T/T_1)^3$$

determines the value of the reduced variable

$$y=-\frac{k_BT}{E_0}\ln\left[\frac{\sigma}{\sigma_1}\right]\ .$$

In these expressions f is a function that depends on the system dimensionality,[20] and the temperature T_1 is determined by the equation

$$(k_BT_1)^3=\pi E_0^4a^3N(E_F)/6P_3\ , \tag{6}$$

where P_3 is the critical number of links connected to a given site.[7] Using the critical exponents obtained by Efros and Shklovskii[22] and the model of Friedman and Pollak[23] for calculating the preexponential factor, the following expression has been proposed by Ortuno and Pollak[8] and used in the present work:

$$\sigma_1=1.7e^2(\nu/a)[a^3N(E_F)]^{0.58}(k_BT)^{-0.42}\ . \tag{7}$$

The Eqs. (6) and (7) involve three physical quantities: ν/a, $a^3N(E_F)$, and the energy parameter E_0, which can be deduced from the best fits of the theory to the experimental data at low and moderate temperatures (Fig. 4). When x increases from 0.47 to 1.0 it is to be noticed that E_0 increases from 0.28×10^{-2} to 2×10^{-2} eV (Fig. 5). This variation is not unexpected, for when the tin content decreases, the optical band gap increases, leading to a density of states which has a tendency to level up. Correlatively the product $a^3N(E_F)$ decreases from 6×10^{-2} to 0.5×10^{-2} eV^{-1} (Fig. 2). This product is about 1 order of magnitude larger than that deduced from Mott's theory, even though its variation with x is quite comparable. Using again $a=10$ Å, $N(E_F)$ changes from 6×10^{19} to 5×10^{18} eV^{-1}cm^{-3} and the frequency ν varies between 3×10^{13} and 10^{14} s^{-1}. Thus the densities of states obtained using Mott's model or percolation theory with a variable density of states agree within a factor of 10. Both models provide values of $N(E_F)$ which increase with tin concentration, showing that the substitution of Sn atoms for Si atoms in the random network produces more localized states in the gap. Simultaneously, incorporation of Sn in the network leads to a softening of the phonon frequencies.

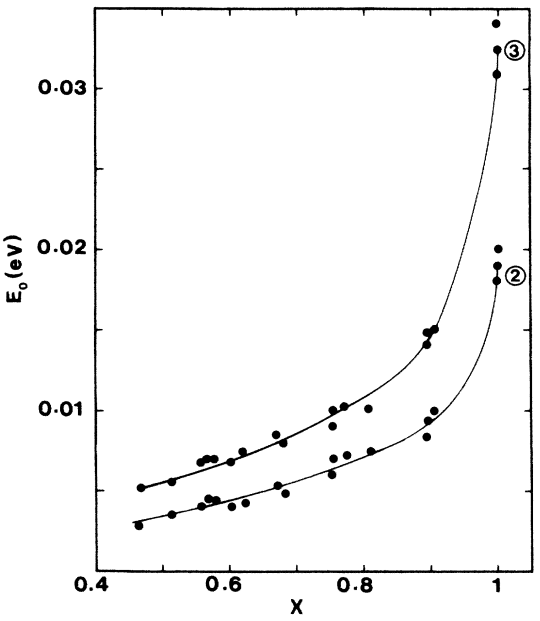

FIG. 5. Variation with x of the energy parameter E_0 involved in the expression of the density of states: $N(E)=N(E_F)\exp(E/E_0)$. 2, Ortuno and Pollak's model; 3, Mott's model with a varying density of states.

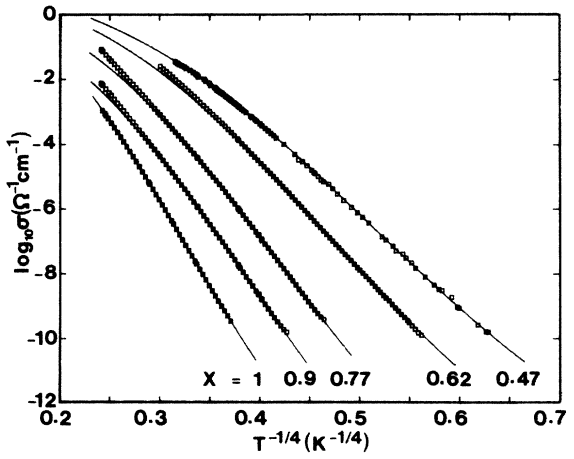

FIG. 4. Variation of $\log_{10}\sigma$ with $T^{-1/4}$ in a-Si_xSn_{1-x} alloys with $x=0.47$, 0.62, 0.77, 0.90, and 1. The continuous lines are best fits of data to Ortuno and Pollak's formula.

3. *VRH theory: variable density of states*

As shown in the preceding paragraph, the percolation model with an exponential density of states accounts fairly well for experimental data, and leads to reasonable values for the physical quantities of interest. With respect to the initial theory of Mott, two new ingredients were introduced: percolation theory and a variable density of states. In order to determine which one is the most important, we introduce now a variable density of states of the form (5) in the VRH treatment of Mott.

The optimal jump frequency

$$\omega=\nu\exp\left[-\frac{2R}{a}-\frac{\Delta}{k_BT}\right]$$

is determined, with the condition that the jump distance R and the energy interval Δ must be related by the equation

$$\tfrac{4}{3}\pi R^3\int_0^{\Delta}N(E_F)\exp(E/E_0)dE=1\ .$$

The optimal jump distance R is therefore given by

$$\frac{2R}{a}(AR^3+1)=3\frac{E_0}{k_BT},$$

with

$$A=\tfrac{4}{3}\pi N(E_F)E_0 .$$

Using this procedure we obtain for the conductivity

$$\sigma=\sigma_2\exp(-\xi), \tag{8}$$

with

$$\sigma_2=0.166e^2(\nu/a)[a^3N(E_F)](R/a)^2$$

and

$$\xi=\frac{2R}{a}+\frac{E_0}{k_BT}\ln\left\{1+\left[\frac{4\pi}{3}E_0[a^3N(E_F)]\left[\frac{R}{a}\right]^3\right]^{-1}\right\}.$$

As in percolation theory this model involves the three parameters $a^3N(E_F)$, E_0, and ν/a. The quality of the fits to experimental data, shown in Fig. 6, is equivalent to that obtained when Ortuno and Pollak's model is used. This observation leads us to the conclusion that a detailed percolation treatment is necessary to resolve the incompatibility between the slope and intercept of the curves representing $\ln\sigma$ versus $T^{-1/4}$, and that the essential ingredient to account for the shape of these curves is the fact that the density of states changes with energy and has a concave curvature.

Using this simple model, we obtained the variation with x of the physical quantities E_0, $a^3N(E_F)$ and ν/a shown in Figs. 5, 2, and 3. E_0 increases from 0.5×10^{-2} to 3.4×10^{-2} eV, the product $a^3N(E_F)$ decreases between 2.3×10^{-2} and 0.24×10^{-2} eV^{-1}, whereas ν/a varies from 3×10^{22} to 7×10^{23} s^{-1} cm^{-1} when x increases from 0.47 to 1.0. If again the value $a=10$ Å is chosen, quite reasonable values for $N(E_F)$ are obtained, between 2×10^{19} eV^{-1} cm^{-3} for $x=0.47$ and 2.5×10^{18} eV^{-1} cm^{-3} for pure silicon. The large values obtained for ν (between 3×10^{15} and 7×10^{16} s^{-1}) can be traced to the approximate optimization procedure used to calculate the optimal jump frequency.

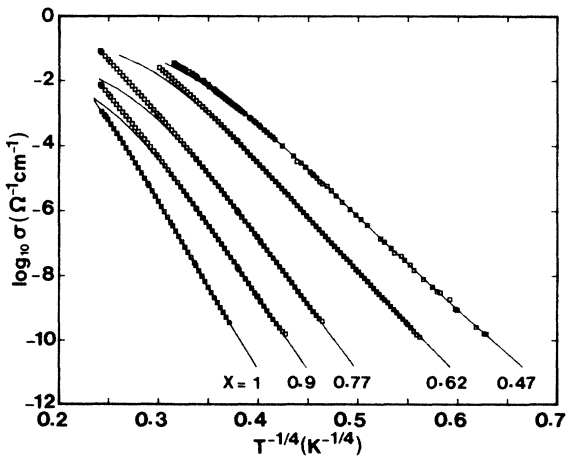

FIG. 6. Variation of $\log_{10}\sigma$ with $T^{-1/4}$ in a-Si_xSn_{1-x} alloys. The continuous lines are best fits of data to Mott's model with a varying density of states.

4. *Effect of annealing treatments*

As the variable-range hopping theory is able to reproduce correctly the experimental data at low and moderate temperature, we used it to interpret the thermal variation of the conductivity observed after annealing at temperatures larger than 300 K. Figure 7 shows the variation of $\log_{10}\sigma$ with $T^{-1/4}$ below 300 K, for amorphous samples with $x=0.75$, 0.9, and 1.0. Each curve is labeled according to the annealing temperature T_a. Again the theory of Ortuno and Pollak allows us to correctly represent the experimental data in a very large range of temperature and composition. The physical quantities obtained from the best fits are recorded in Table I.

The energy parameter E_0 increases slightly when the annealing temperature is enhanced. This again can be explained by a flattening of the density of states curve, due to the fact that the optical band gap increases on annealing.[24,25] A peculiarity of the results recorded in Table I is that the product $a^3N(E_F)$ does not change much with annealing temperature T_a, whereas $N(E_F)$ is expected to decrease. This can be qualitatively explained as follows. The energy of a localized level depends on its local environment. It is likely that strongly perturbed regions of the sample are connected with deep energy levels (of small localization length).

It is also possible that the atomic mobility of these constrained configurations is relatively high. According to this assumption, deep levels, i.e., levels with the smallest localization length, would be observed to anneal first, so

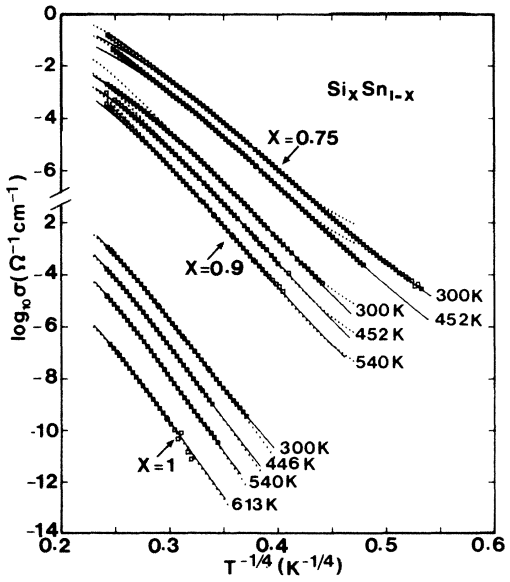

FIG. 7. Change of $\log_{10}\sigma$ with $T^{-1/4}$ as a function of the annealing temperature (indicated in the figure). Solid and dotted lines, respectively, represent the fits obtained using the Ortuno and Pollak theory or the small-polaron theory.

TABLE I. Variation of $a^3N(E_F)$, E_0, and ν/a with annealing temperature T_a, for amorphous Si_xSn_{1-x} alloys, according to the model proposed by Ortuno and Pollak (Ref. 8).

x	T_a (K)	$a^3N(E_F)$ (10^{-2} eV^{-1})	E_0 (10^{-2} eV)	ν/a (10^{20} s^{-1}cm^{-1})
1	300	0.53	2.0	14.2
	446	0.41	2.1	3.60
	540	0.36	2.25	0.582
	613	0.35	2.3	0.013
0.9	300	1.15	0.85	3.60
	452	0.96	1.00	2.45
	540	0.77	1.20	1.38
0.75	300	2.0	0.6	3.54
	452	1.8	0.66	1.96

that the average localization length of the remaining defects would increase with increasing annealing temperature T_a. The strong variation of ν/a for pure amorphous silicon can be ascribed to uncertainties in the preexponential factor.

B. Small-polaron model

As recalled in the Introduction, it has been suggested that the disorder in amorphous alloys may trigger the formation of small polarons. The polaron mobility has been studied in detail by Holstein in crystalline systems,[26] and by Emin[5,9] and Gorham-Bergeron and Emin[10] in disordered alloys. Viscor[11] used the high-temperature approximation to interpret dc conductivity data obtained in amorphous germanium. In what follows we investigate the ability of this theory to account for the thermal variation of the dc conductivity in our Si_xSn_{1-x} amorphous alloys.

Including the coupling of carriers with optical and acoustical phonons leads to the following formula for the jump frequency between two sites:

$$\omega=\left[\frac{J}{\hbar}\right]^2\left[\frac{\pi\hbar^2}{2(E_c^o+E_c^a)k_BT}\right]^{1/2}\times\exp\left[-\frac{\Delta^2}{8(E_c^0+E_c^a)k_BT}\right]\times\exp\left[-\frac{\Delta}{2k_BT}\right]\exp\left[-\frac{E_A^o}{k_BT}\right]\exp\left[-\frac{E_A^a}{k_BT}\right],$$

where J is the transfer integral between the localized wave functions centered on sites whose energy difference is Δ. The energies E_c^o, E_c^a and E_A^o, E_A^a are defined in Ref. 10. They involve the contribution, to the polaron binding energy, of the interaction of a carrier with optical (o) or acoustical (a) phonons. The phonon spectra are determined by ω_o, the average optical frequency, and ω_D the Debye frequency.

Following Viscor[11] we may assume that, once formed, the polaron can jump towards every site in the amorphous sample. Polaronic jumps are thus expected to occur between next-neighbor sites, separated by the average distance d, so that we can write

$$J=J_0\exp(-d/a),$$

where a is the range of the localized wave function. It is also expected that Δ is small because the local atomic structure of polaronic sites, in the random continuous network, varies little from site to site. These remarks lead to the high-temperature approximation to the jump frequency ω proposed by Viscor,[11]

$$\omega=\left[\frac{J_0}{\hbar}\right]^2\exp\left[-\frac{2d}{a}\right]\left[\frac{\pi\hbar^2}{2(E_c^o+E_c^a)k_BT}\right]^{1/2}\times\exp\left[-\frac{E_A^o}{k_BT}\right]\exp\left[-\frac{E_A^a}{k_BT}\right]. \quad (9)$$

From this expression we calculate the conductivity using the Einstein relation:

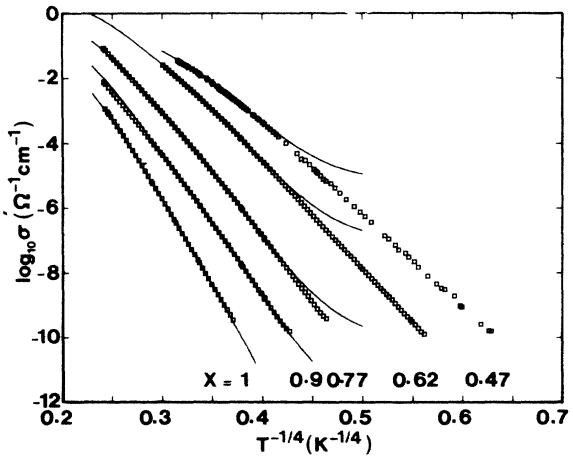

FIG. 8. Best fits of the experimental data to the small-polaron theory (high-temperature approximation) in a-Si_xSn_{1-x} amorphous alloys.

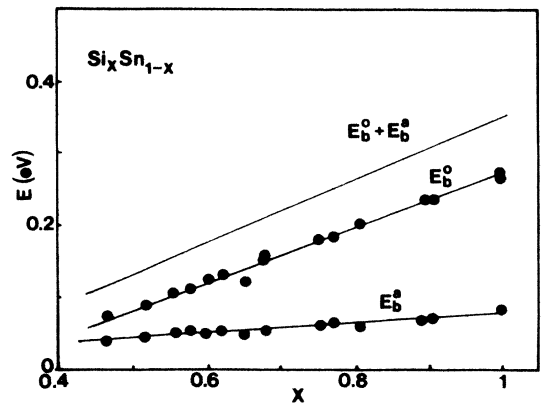

FIG. 9. Variation with x of the energy parameters E_b^o and E_b^a involved in the small-polaron model.

TABLE II. Small-polaron model. Variation of $E_b^o+E_b^a \sim E_g/4$ and of J^2N_c with the annealing temperature T_a in amorphous Si_xSn_{1-x} alloys.

x	T_a (K)	$(E_b^o+E_b^a)$ (eV)	J^2N_c (10^{17} eV^2 cm^{-3})
1	300	0.35	4.6
	446	0.367	1.0
	540	0.381	0.14
	613	0.385	2.8×10^{-3}
0.9	300	0.305	8.1
	452	0.320	3.3
	540	0.332	0.73
0.75	300	0.242	46.3
	452	0.251	23.0

$$\sigma=\frac{1}{6k_BT}N_ce^2\omega d^2 ,$$

where N_c is the carrier concentration. In order to interpret our data, the energies E_c^o, E_c^a and E_A^o, E_A^a which depend on the energies E_b^o and E_b^a defined in Ref. 10 have been evaluated assuming that $\Delta_b/2=E_b^o+E_b^a=E_g/4$, where E_g is the optical gap, obtained through optical absorption measurements.[19] The frequencies ω_D and ω_0, determined by Mössbauer spectroscopy on the ^{119}Sn nucleus,[17] do not vary much with the alloy concentration. The following average values have been chosen in our analysis: $\omega_D=2.1\times10^{13}$ and $\omega_0=8.1\times10^{13}$ s^{-1}. The distance d between neighboring sites has been estimated using the equation

$$d=xd_{\text{Si-Si}}+(1-x)d_{\text{Sn-Sn}} ,$$

with $d_{\text{Si-Si}}=2.35$ Å and $d_{\text{Sn-Sn}}=2.80$ Å.

Using these values for the relevant parameters in the theory, the calculated values of σ represent very well the experimental data for all temperatures larger than about 30 K (Fig. 8).

The agreement between experiment and theory is slightly better if we consider that ω_D, ω_0, E_b^o, and E_b^a, are adjustable parameters but again the agreement is only observed for $T>30$ K. Using this procedure we obtained values for E_b^o and E_b^a as a function of x (Fig. 9). Whatever the alloy composition, it appears that the coupling to optical phonons is more effective than to acoustical phonons.

Figure 10 shows that the product N_cJ^2 obtained from the preexponential factor in the expression of σ varies parabolically with x, and shows a maximum near $x=0.75$. Using the estimate value $J=0.02$ eV[11], this provides values of N_c between 5×10^{20} and 10^{22} cm^{-3}.

The behavior of the conductivity after annealing has also been discussed using the small-polaron model. The frequencies ω_0 and ω_D were considered independent of the annealing temperature and the ratio E_b^o/E_b^a was kept constant so that the only adjustable parameters were $E_b^o+E_b^a$ and N_cJ^2. The fits to the experimental data are shown as dotted curves in Fig. 7 and the values obtained for the parameters are given in Table II.

As shown in Table II, the sum $E_b^o+E_b^a=E_g/4$ increases on annealing and the product J^2N_c decreases strongly. This result is consistent with the annihilation of defects on annealing[27] and with the increase of the optical gap.[24,25]

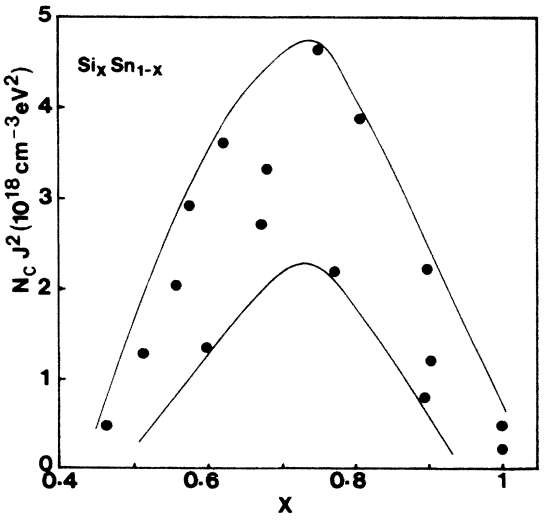

FIG. 10. Variation of N_cJ^2 with x in the small-polaron model. N_c is the carrier concentration and J is the transfer integral.

IV. CONCLUSION

In this paper we have presented a systematic experimental study of the variation of the dc conductivity of amorphous Si_xSn_{1-x} alloys as a function of temperature and composition, and after annealing treatments. The results have been interpreted using variable-range hopping models and the small-polaron theory.

The first category of models is shown to agree well with experimental data, even for temperatures as low as 6 K in alloys with large tin concentration. The small-

polaron model, in the version proposed by Viscor, correctly represents the data above 30 K, but departs from experiment at low temperature. This failure was not apparent in previous works devoted to pure amorphous semiconductors because the lowest possible temperature for which conductivity measurements were feasible was of the order of 20–30 K. A result of the present work is that the polaron theory, in its high-temperature approximation, is not adequate for temperatures smaller than about 30 K in the amorphous alloys investigated here.

Various VRH models have been tried to interpret the experimental data. These models involve two essentially different ingredients: the intrinsic variation of the density of states and the percolation process. It has been shown that the VRH treatment proposed by Mott, with an exponentially variable density of states, accounts fairly well for experimental observations. The percolation theory proposed by Ortuno and Pollak agrees even better with experiment, in that the discrepancy between the values of $N(E_F)$ deduced from the slope and intercept of the traces of $\ln\sigma$ versus $T^{-1/4}$ largely disappears.

ACKNOWLEDGMENTS

We would like to thank Professor Sir Nevill Mott for enlightening discussions and Dr. M. L. Theye and A. Mohamedi for their contribution to the optical measurements. The Laboratoire de Physique du Solide is "Unité associée au Centre National de la Recherche Scientifique No. 155."

[1]N. F. Mott and E. A. Davis, *Electronic Processes in Non-Crystalline Materials* (University Press, Oxford, 1979).

[2]P. N. Butcher, in *Amorphous Solids and the Liquid State*, edited by N. H. March, R. A. Street, and M. Tosi (Plenum, New York, 1985), p. 311.

[3]B. I. Shklovskii and A. L. Efros, *Electronic Properties of Doped Semiconductors* (Springer-Verlag, Berlin, 1984).

[4]P. G. Le Comber and W. E. Spear, in *Amorphous Semiconductors*, edited by M. H. Brodsky (Springer-Verlag, Berlin, 1979), p. 251.

[5]D. Emin, Comments Solid State Phys. **11**, 35 (1983).

[6]A. Miller and E. Abrahams, Phys. Rev. **120**, 745 (1960).

[7]M. Pollak, in *The Metal-Non-Metal Transition in Disordered Systems*, edited by L. Friedman and D. P. Tunstall (SUSSP, Edinburgh, 1978), p. 95.

[8]M. Ortuno and M. Pollak, J. Non-Cryst. Solids **59-60**, 53 (1983); Philos. Mag. B **47**, L93 (1983).

[9]D. Emin, Phys. Rev. Lett. **32**, 303 (1974).

[10]E. Gorham-Bergeron and D. Emin, Phys. Rev. B **15**, 3667 (1977).

[11]P. Viscor, Phys. Rev. B **28**, 927 (1983); Solid State Commun. **32**, 281 (1979).

[12]G. P. Triberis and L. R. Friedman, J. Phys. C **14**, 4631 (1981); **18**, 2281 (1985).

[13]M. L. Knotek, Solid State Commun. **17**, 1431 (1975).

[14]M. L. Knotek, M. Pollak, T. M. Donovan, and H. Kuntzman, Phys. Rev. Lett. **30**, 853 (1973).

[15]M. Vergnat, G. Marchal, M. Piecuch, and M. Gerl, Solid State Commun. **50**, 237 (1984).

[16]M. Vergnat, M. Piecuch, G. Marchal, and M. Gerl, Philos. Mag. B **51**, 327 (1985).

[17]M. Vergnat, M. Piecuch, J.-F. Gény, C. Mourey, G. Marchal, and M. Gerl, Proceedings of the Third Congress on Structure of Non-Crystalline Materials, [J. Phys. (Colloq.) 8 **46**, 287 (1987)].

[18]N. Maloufi, A. Audouard, M. Piecuch, and G. Marchal, Phys. Rev. Lett. **56**, 2307 (1986).

[19]A. Mohamedi (private communication).

[20]N. Maloufi, Doctorate thesis, University of Nancy I, 1986.

[21]M. Abkowitz, P. G. Le Comber, and W. E. Spear, Commun. Phys. **1**, 75 (1976).

[22]A. L. Efros and B. I. Shklovskii, in *Electronic Phenomena in Non-Crystalline Semiconductors*, edited by B. T. Kolomiets (Nauka, Leningrad, 1975).

[23]L. Friedman and M. Pollak, Philos. Mag. B **44**, 487 (1981).

[24]M. L. Theye, in *Proceedings of the 5th International Conference on Amorphous and Liquid Semiconductors, Garmisch-Partenkirchen, 1973*, edited by J. Stuke and W. Brening (Taylor and Francis, London, 1974), p. 479.

[25]P. J. Elliott, A. D. Yoffe, and E. A. Davis, in *Tetrahedrally Bonded Amorphous Semiconductors*, Proceedings of the International Conference on Tetrahedrally Bonded Amorphous Semiconductors, AIP Conf. Proc. No. 20, edited by M. H. Brodsky, S. Kirkpatrick, and D. Weaire (AIP, New York, 1974), p. 311.

[26]T. Holstein, Ann. Phys. (N.Y.) **8**, 325 (1959); **8**, 343 (1959).

[27]A. Por, A. Audouard, M. Gerl, G. Marchal, and N. Maloufi, Solid State Commun. (to be published).